Springer

KSME

Journal of Mechanical Science and Technology 32 (8) (2018) 3699~3706
www.springerlink.com/content/1738-494x(Print)/1976-3824(Online)
DOI 10.1007/s12206-018-0722-7

An experimental loading study of a pitching wind turbine airfoil in near- and post-stall regions †

Mehran Masdari*, Mahbod Seyednia and Arshia Tabrizian

Faculty of New Sciences and Technologies, University of Tehran, Tehran, Iran

(Manuscript Received January 5, 2018; Revised April 13, 2018; Accepted April 29, 2018)

Abstract

A series of experimental tests was conducted to present an insight into lift characteristics of an oscillating wind turbine airfoil at near- and post-stall regions. Due to the unsteady nature of the flow around a wind turbine, the blades are subjected to oscillating motions and consequently, unsteady phenomena occur, dynamic stall in particular. Therefore, the unsteady lift of wind turbine blades is of considerable importance in performance and estimation of a wind turbine lifespan. In the current study, at Re = 420000, a detailed survey of parameters affecting lift characteristics in the hysteresis loops are carried out for the critical section of a 660 kW wind turbine blade. To investigate the effects of reduced frequency, mean angle of attack (AOA) and amplitude of oscillation, the characteristics of lift hysteresis loops including maximum lift, width of the loop, crossover point (if exists) and the normal force defect (NFD) are compared qualitatively and quantitatively. The results indicate that increase of reduced frequency leads to decrease in lift curve slope and delay in maximum lift occurrence. Furthermore, the lift curves are the evidence of strong dependence of lift characteristics on mean AOA and amplitude of pitching motion. Increase of amplitude makes the airfoil enter the post-stall region and hence, it delays the maximum lift occurrence. Entering the post-stall region, the airfoil encounters deeper dynamic stall. Also, approaching to post-stall region makes the clockwise part of the loops more dominant.

Keywords: Dynamic stall; Experimental unsteady aerodynamics; Normal force defect; Wind turbine airfoil

1. Introduction

Horizontal axis wind turbines (HAWT) are subjected to unsteady flows during their operation periods. The unsteadiness originates from periodic and aperiodic flowfield structures such as wind speed, wind turbulence, tower shadow, yaw errors, blade/wake interactions and so on [1, 2]. These substantially affect the aerodynamic characteristics of wind turbine blades. The unsteady behavior of a wind turbine blade comes into existence in the form of some basic blade motions including pitch, plunge or the combination of both. Furthermore, flow separation and dynamic stall are inherent unsteady phenomena occurring due to the unsteady behavior of the flow around wind turbine blades which are the primary sources of fatigue and failure in wind turbine components [3].

Due to the important impact of unsteady phenomena on performance of wind turbines, dynamic stall in particular, unsteady aerodynamics has attracted a number of studies during last three decades. While an airfoil experiences a pitching or plunging motion, dynamic hysteresis occurs in aerodynamic coefficients. When the flow is separated and a vortex known as dynamic stall vortex (DSV) forms on the surface of the airfoil, the convection of the DSV into the downstream leads to dynamic stall and consequently, it presents a large hysteresis on lift coefficient loop. Under the dynamic stall effects, the stall angle of an airfoil is found to be higher than the normal static stall angle. In unsteady conditions, the lift force can still be maintained even at angles of attack (AOA) higher than static stall angle.

The beginning of analysis of unsteady aerodynamics can be attributed to Theodorsen [4] in 1935 where he theoretically modeled the unsteady lift of an airfoil in motion at fully-attachment condition. He predicted dynamic hysteresis of aerodynamic coefficients due to the phase lead of noncirculatory effects and the phase lag due to vorticity convection into the wake. The main researches on dynamic stall and airfoils in motion, however, started in the 1970s and early 1980s by McAlister et al. [5] and McCroskey et al. [6]. They conducted a series of experimental analysis of dynamic stall phenomenon in pitching airfoils. In the 1980s, McCroskey carried out a thorough physical analysis of dynamic stall in two review papers [7, 8]. Since then, several experimental study [9-13] alongside numerical analyses [14-17] have been conducted to

*Corresponding author. Tel.: +98 9126219381, Fax.: +98 21 88056527
E-mail address: m.masdari@ut.ac.ir
† Recommended by Associate Editor Hyoung-Bum Kim

investigate the unsteady behavior of airfoils in motion and dynamic stall phenomenon. Among them, different airfoil geometries, flow regimes, Reynolds number and motion conditions with different applications can be found in the literature.

Although the modern HAWT may operate in the range of high-Reynolds number, the small-medium turbines work in the range of moderate-Reynolds number (10^5) generally. The flow structure in this regime is highly nonlinear [18], and the dynamic stall occurs according to the vortex formation on the upper surface and the transition of laminar flow to turbulent in boundary layer. There exists very few studies in the literature, either numerically or experimentally, concerning the pitching airfoils in moderate-Reynolds number regime [11, 19-22]. Also, several active and passive control methods have been implemented on airfoils to alleviate or control the loads on wings and blades [14, 23, 24]. The scope of the current work, however, is to experimentally investigate the detailed unsteady phenomena occurring in pitching motion of a wind turbine airfoil, regardless of controlling the flow around. Although many unsteady phenomena contributing to wind turbine blades behavior are known, the details of dynamic stall and pitching oscillation are still state of the art. Today, due to computational limitations [17, 20, 25], there is a growing demand for more experimental analysis of unsteady phenomena either in aeronautical applications or wind turbine industry. Besides, the reliability and remarkable accuracy of experimental data encourage the researchers to extend experimental studies, particularly in post-stall region where numerical simulations can hardly capture the physics of flow.

In the current study, we thoroughly investigate the parameters affecting the unsteady behavior of a harmonically oscillating wind turbine airfoil at near- and post-stall regions. The parameters discussed herein include reduced frequency, mean AOA and amplitude of oscillation. The values of these parameters are selected in a way that the airfoil undergoes pitching motion in near- and post stall regions where critical and destructive loads can be imposed on a wind turbine blade. The influence of these parameters on the maximum lift coefficient in hysteresis loops, the position of crossovers in lift hysteresis (if exists) and the normal force defect (NFD) are studied. By comprehensive investigation of these parameters on dynamic stall, one can have more insights into the physics of unsteady aerodynamics around an oscillating wind turbine airfoil. The experimental apparatus and test conditions are presented in Sec. 2. The results and discussion are provided in Sec. 3. At the end, in Sec. 4, the summary and conclusions are presented.

2. Experimental apparatus and tests

The experimental tests were carried out in a low-speed closed circuit wind tunnel with a rectangular test section of 0.8 × 0.8 × 2 m. The maximum air speed of 100 m/s can be attained in the test section which limits the Reynolds number to Re = 1400000 for an airfoil with a chord length of c = 0.25 m.

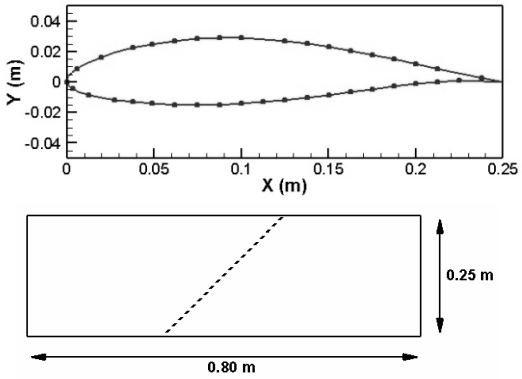

Fig. 1. Airfoil geometry and location of the pressure ports.

The contraction ratio of the tunnel is 7:1 where four large anti-turbulence screens and honeycombs are embedded in the settling chamber to maintain the turbulence intensity of the test section below 0.1 %.

The airfoil model considered in this research is extracted from the critical section of a 660 kW HAWT blade at a distance of 74 % from the root of the blade. This section was selected based on a blade element momentum (BEM) calculation which was performed on the blade. The BEM results showed that the critical load was imposed on the section of 74 % away from the root. Therefore, analysis of this section assures the resistance of other sections against destructive loads. The chord length of the model is 0.25 m with 0.8 m span. For surface pressure measurement, 64 pressure orifices are located on the upper and the lower surfaces of the airfoil model. To diminish the effect of upstream pressure tabs, the tabs are mounted in a line which has a 20 degree angle with the chord line of the model. The geometry of the airfoil and the location of the pressure orifices are depicted in Fig. 1.

Due to the space limitations inside the model, the pressure transducers are located outside the tunnel and they are connected to the pressure ports by tubes. Hence, a series of experiments was carried out to ensure the proper frequency response of the pressure measuring system is maintained for high oscillation frequencies. The tubes are selected in a way that the maximum time lag of the data acquisition is less than 0.01 s. This is equivalent to the frequency response of greater than 100 Hz including the physical features of the tubes. Using a 64 channel, 12 bit A/D board and a terminal board, the transducer data are collected at the rate of 100 Hz. and dispatched to a computer.

The oscillating mechanism implemented in this survey is depicted in Fig. 2. As seen, the pitch mechanism utilizing an AC motor controlled by a proper drive.

The motor is linked to a crank system in order to translate the unidirectional rotation to reciprocating rotation motion. The length of the connecting rod between the motor shaft and airfoil determines the mean AOA of the motion. Meanwhile, the value of off-center connection of the connecting rod to the motor shaft sets the amplitude of the motion. A digital shaft

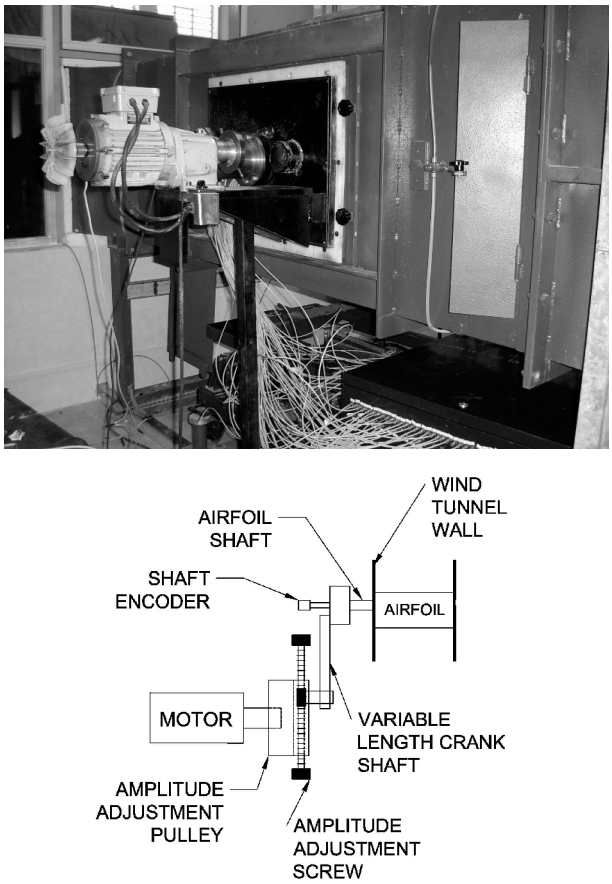

Fig. 2. Pitching oscillation mechanism – the real system and the schematic of the oscillation mechanism.

encoder is aligned to the model shaft providing the instantaneous AOA of the airfoil.

The airfoil has a pitching motion around the quarter chord under the equation below:

$$\alpha = \alpha_0 + d\sin(2\pi ft) \tag{1}$$

where α_0 is the mean AOA, d is the amplitude, ranging from 2 to 11 degrees and f represents the frequency of the motion, ranging from 0.6 to 4 Hz in this research. The range of the frequency corresponds to the reduced frequency ($k = \omega C/2U$) of 0.015 to 0.1 including the quasi-steady and unsteady motions of the airfoil. The freestream velocity in the tests is set to 30 m/s corresponding to the Reynolds number of 420000. The aim of this survey is to investigate the unsteady behavior of the wind turbine airfoil in a pitching motion, ranging from near-stall to post-stall regions. Studying the effects of amplitude, reduced frequency and mean AOA on the physics of dynamic stall and aerodynamic loads on rotor blades in these regions can improve the performance of a wind turbine and enhance the lifespan of the blades. Furthermore, the limitation due to the oscillation system leads to selection of the following values. Table 1 represents the test cases studied in near- and post-stall regions.

Table 1. Test plan.

Region	α_0 (°)	d (°)	k
Near-stall region	5-10	5	0.045
	5	8	0.02-0.045-0.065-0.1
	8	2-5-8	0.1
	13	2	0.1
Post-stall region	8	11	0.015-0.03-0.045-0.1
	10-18	8	0.045
	13	5-8-11	0.1
	18	5	0.025-0.045-0.065-0.1

Based on Eq. (1), the airfoil has a purely sinusoidal pitching motion. The hysteresis effect in this motion can be quantified by calculating a parameter named NFD (ξ). The hysteresis effect in an unsteady motion is in contrast to steady or quasi-steady condition of an airfoil where the flow field adjusts itself with any change in AOA. The NFD, as a quantitative parameter representing the degree of hysteresis, is obtained from the closed line integral around the cycle of the normal force [5] as

$$\xi = \frac{\oint_{\pi/2} C_n d\alpha}{\int_{-\pi/2} C_n d\alpha}. \tag{2}$$

The NFD represents the loss in load carrying ability due to the downstroke motion of the airfoil. So, the denominator of the Eq. (2) represents the area under the curve in normal force coefficient versus AOA diagram in upstroke motion and the integral in the numerator calculates the area of the C_n-α hysteresis loop.

The NFD value in lift curves with crossover point determines whether the dominant phase of motion is lead or lag with respect to static lift curve. The positive values of NFD represent the dominant lead phase while the negative ones show the dominant lag phase. Where no crossover point exists, however, the NFD absolute value indicates the width of the hysteresis loops.

The uncertainty analysis of the collected data using sum square of both bias and precision errors revealed the maximum error of 2 % in lift coefficient.

3. Results and discussion

The effects of reduced frequency, mean AOA and amplitude in the pitching motion of the mentioned airfoil at near- and post-stall regions are discussed in the following. The time behavior of the measured lift values are thoroughly analyzed and the lift coefficient loops for all cases are plotted. The arrows in the lift coefficient diagrams represent the direction of the airfoil motion.

In addition, according to the lift hysteresis loops, the values of maximum lift and crossover point (if exists) are specified

for better comparison. The solid circles on the lift hysteresis loops represent the crossover points. Moreover, based on Eq. (2), the NFDs are calculated in each case and the results are plotted as well. Also, the table in each section gives a summary of the characteristics of the lift curves.

3.1 Effect of reduced frequency

Three different cases with different mean AOAs and amplitudes are considered to investigate the effect of reduced frequency on the dynamic hysteresis of lift coefficient for the pitching airfoil. The cases are selected in a way that the results will cover the near- and post-stall regions in quasi-steady and unsteady flows. Fig. 3 represents the lift coefficient loops of three cases at different reduced frequencies.

Fig. 3(a) corresponds to the airfoil motion in the near-stall region where the mean AOA is 5° and the amplitude is 8°. It is noticeable that increase of reduced frequency slightly widens the hysteresis loops and simultaneously, declines the slope of the curves. Also, the crossover point, representing the so-called "Fig. 8" occurrence, moves forward with growth of reduced frequency which represents the faster reattachment of the flow in downstroke motion. The "Fig. 8" represents the intersection in lift hysteresis where in downstroke motion, the lift values exceed the corresponding values in upstroke motion. This can be attributed to either the reattachment of flow to the upper surface in downstroke motion or the existing vortex previously formed in high AOAs.

In the second case where the mean AOA and the amplitude are 8° and 11°, respectively (Fig. 3(b)), the increase of reduced frequency leads to delay in maximum lift occurrence in upstroke motion. The displacement of crossover point is similar to the first case where it moves forward with growth of the reduced frequency. Furthermore, the drop of the lift value at the end of upstroke motion decreases in the highest reduced frequency, while in other cases the drop is negligible. It suggests the lighter dynamic stall occurrence for higher reduced frequencies at near- and post stall regions where the flow is not fully separated.

For the case of mean AOA = 18° and the amplitude of 5° (Fig. 3(c)), it is clearly noticeable that the lift coefficient loops of all the reduced frequencies are clockwise, representing the lead phase of the flow with respect to the static one. For all reduced frequencies, the flow in downstroke motion is not fully-reattached and consequently, no intersection in lift loops happens. Herein, the airfoil oscillates at post-stall region and consequently, the generated lift is mostly due to higher apparent mass at higher reduced frequencies where no specific pattern exists for circulatory part of lift. As a result, the width of the loops grows by increase of reduced frequency. The maximum lift of the curves for different reduced frequencies does not change drastically and all the values are lower than the value of maximum lift in Figs. 3(a) and (b). Such a feature in lift hysteresis is actually related to the separated flow at high AOAs.

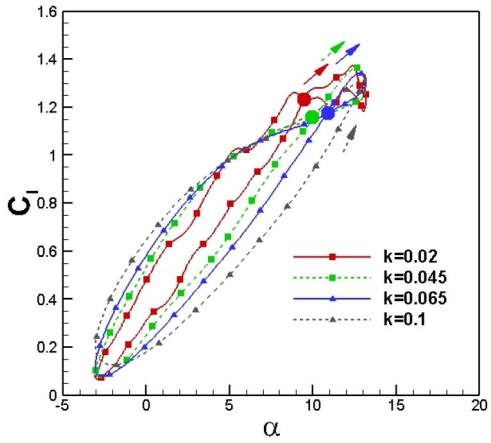

(a)

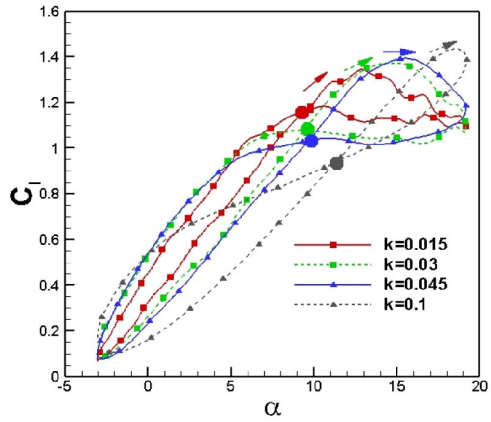

(b)

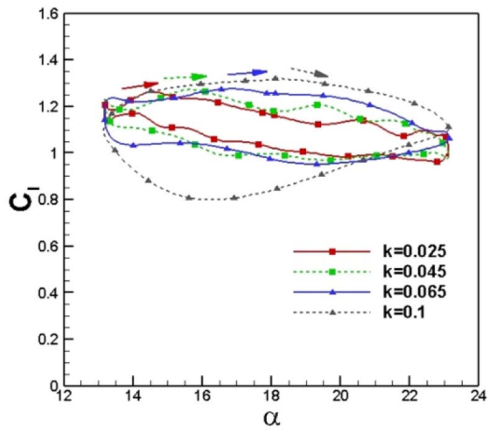

(c)

Fig. 3. Effect of reduced frequency: (a) Mean AOA = 5°, d = 8°; (b) mean AOA = 8°, d = 11°; (c) mean AOA = 18°, d = 5°.

The values of the NFD are calculated for all cases and can be seen in Table 2. For better comparison, the NFD for three cases are plotted in Fig. 4. According to Fig. 3(a), it can be seen that the dominant part of the hysteresis loops are counter-clockwise and hence, the NFD value is negative. The magnitude of the NFD increases by the growth of reduced frequency.

Table 2. Effect of reduced frequency on lift characteristics.

α_0 (°)	d (°)	k	Crossover point (°)	Max. C_l	NFD
5	8	0.02	9.52	1.369	-13.78
5	8	0.045	10.06	1.367	-25.41
5	8	0.065	10.83	1.346	-38.49
5	8	0.1	-	1.341	-66.51
8	11	0.015	9.29	1.347	-2.55
8	11	0.03	9.47	1.373	-3.90
8	11	0.045	9.75	1.399	-4.87
8	11	0.1	11.45	1.442	-17.73
18	5	0.025	-	1.268	10.50
18	5	0.045	-	1.272	14.19
18	5	0.065	-	1.276	17.56
18	5	0.1	-	1.319	27.74

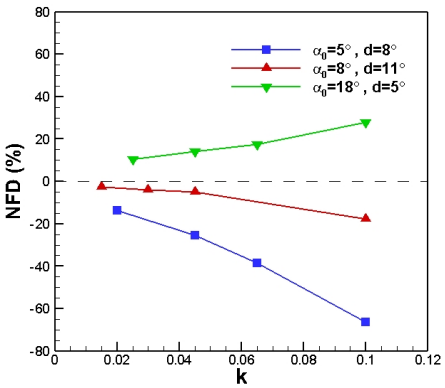

Fig. 4. NFD vs. reduced frequency for three different cases.

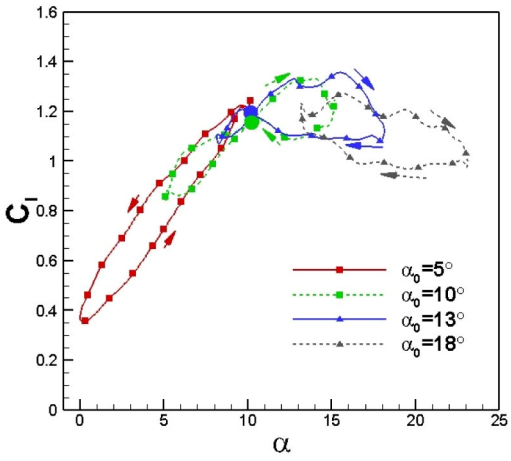

(a)

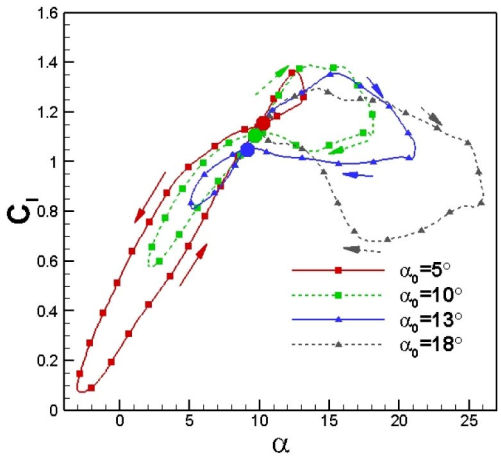

(b)

Fig. 5. Effect of mean AOA: (a) d = 5°, k = 0.045; (b) d = 8°, k = 0.045.

The increase of reduced frequency leads to the vanishing of the current light dynamic stall occurrence and therefore, the width and the area of the counterclockwise part expands.

As seen in Figs. 3(a) and (b), at the onset of post stall region, the area of the clockwise part expands and the value of the NFD approaches to positive values. In the case of mean AOA = 18° and D = 5° (Fig. 3(c)), due to phase lead of noncirculatory effects, the hysteresis loops are totally clockwise and according to Fig. 4, the width of the curves and consequently, the NFD increase by increase of reduced frequency.

3.2 Effect of mean AOA

Increasing the mean AOA with constant amplitude of oscillation (5° and 8°) leads to entrance to the separation and hence, the stall regions. Based on the reduced frequency of 0.045 considered herein, at pre-stall region with mean AOA of 5° and the amplitude of 5° (Fig. 5(a)), no separation occurs and the phase lag due to circulatory effects makes the lift hysteresis totally counterclockwise. For the corresponding case in Fig. 5(b), however, increasing the amplitude to 8° makes the airfoil encounter light stall due to slight drop of lift coefficient at the end of upstroke motion. Regarding the direction of hysteresis loop, the lift hysteresis of mean AOA = 18° for both amplitudes, by contrast, is completely clockwise. This corresponds to the dominant phase lead of the lift with respect to the airfoil motion at fully stall region. In between, at near-stall region, the phase lag of lift turns to phase lead in upstroke motion. So, the so-called "Fig. 8" shape occurs in lift hysteresis.

For both amplitudes, the increase of mean AOA makes the airfoil be at near- and post-stall regions and consequently, the airfoil encounters dynamic stall phenomenon. As a result, the slope of the curves are declining by entering the stall regions. Figs. 5(a) and (b) suggest that in the higher amplitude of oscillation, 8°, deeper dynamic stall occurs. Also, the crossover point moves backward representing that due to the deeper dynamic stall occurrence, the flow reattachment to the airfoil surface delays in downstroke motion.

As seen in Fig. 6, initially, the values of the NFD for both cases are negative. This is due to the dominant counterclockwise part in lift hysteresis loops in near stall regions. However, increase in reduced frequency makes the clockwise part more

Table 3. Effect of mean AOA on lift characteristics.

α_0 (°)	d (°)	Crossover point (°)	Max. C_l	NFD
5	5	-	1.359	-19.87
10	5	9.78	1.381	2.45
13	5	10.27	1.354	10.58
18	5	-	1.292	14.19
5	8	10.01	1.254	-25.41
10	8	9.81	1.327	5.43
13	8	8.95	1.353	13.50
18	8	-	1.271	26.84

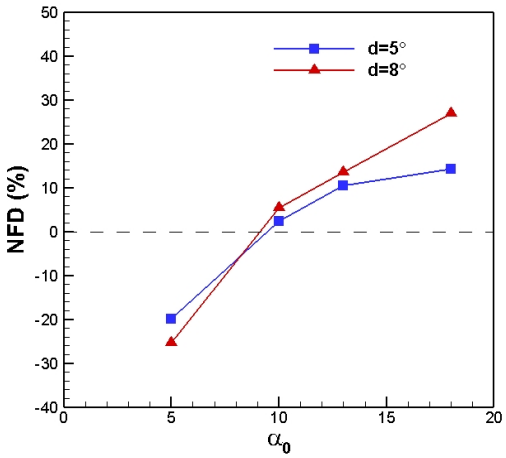

Fig. 6. Normal force defect vs. mean AOA for two different cases.

dominant and therefore, the values of NFD increases as well. More interestingly, the slope of the NFD curves in Fig. 6 is decreasing which can be attributed to the nonlinear physics of dynamic stall occurrence and consequently, the nonlinear increase of hysteresis width with increase of mean AOA.

3.3 Effect of amplitude

In this section, the amplitude of the oscillation varies over the range of 2° to 11° for constant mean AOA of 8° and 13°. The reduced frequency of the oscillations is 0.1 which represents the unsteady flow around the airfoil. As shown in Figs. 7(a) and (b), the increase of the oscillation amplitude enhances the unsteadiness of the flow and consequently, widening the hysteresis loops. The figures suggest that little deviation in lift curve slopes occurs by increase of the amplitude. This can be attributed to the constant reduced frequencies for all the lift curves. The increase of reduced frequency results in a lag in lift rise and reduces the lift slope. So, in this case, the slope remains nearly constant. Additionally, the increase of the amplitude shifts the lift curves downward (with constant slope). This can be attributed to the portion of the attached-flow area on the upper surface of the airfoil which would be shortened by increase of amplitude.

The maximum lift coefficient, however, delays to higher

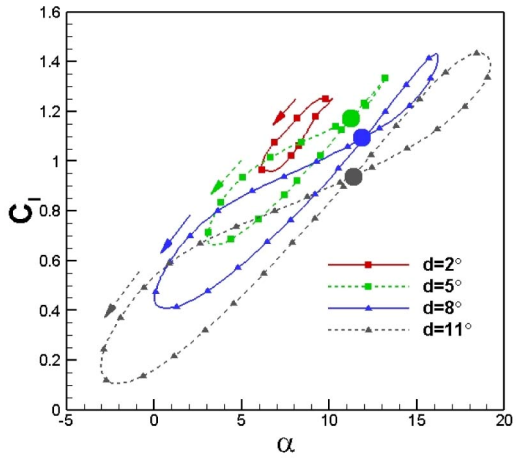

(a)

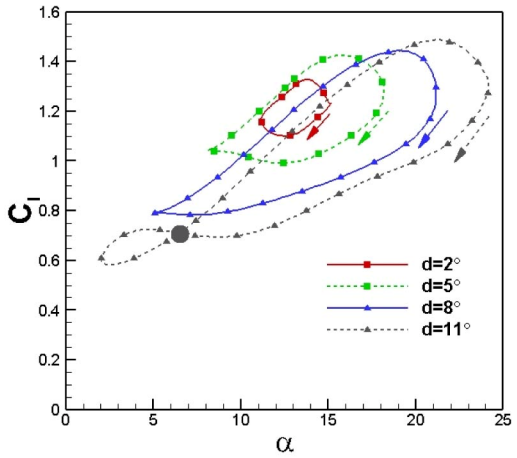

(b)

Fig. 7. Effect of amplitude: (a) α0 = 8, k = 0.1; (b) α0 = 13°, k = 0.1.

AOAs in upstroke motions. As well as the stall AOA, the value of maximum lift coefficient increases by increase of the amplitude. According to Fig. 7(a), the high reduced frequency of the oscillation leads to no abrupt change in the lift coefficient at the end of upstroke motion (even with amplitude of 11°), while at mean AOA of 13°, the increase of the amplitude shows more effective changes in lift. Hence, deeper dynamic stall conditions are encountered by the airfoil.

As seen in Fig. 7, the maximum lift coefficient moves forward for higher amplitude of rotation. The value of maximum lift is slightly enhances by increase of amplitude. This can be attributed to delay in separation and DSV motion in higher amplitude due to high reduced frequency.

Fig. 8 depicts the change in the NFD values for different amplitude of oscillation in both cases. When the mean AOA is 8° and k = 0.1, the airfoil oscillates in a region far away from dynamic stall region. Therefore, the circulatory effects make the flow mostly lag the airfoil motion and consequently, the counterclockwise part would be dominant in hysteresis loops. The increase of amplitude leads to growth in the magnitudes of the NFD. As seen in Fig. 8, the slope of the curve, however,

Table 4. Effect of amplitude on lift characteristics.

α_0 (°)	d (°)	Crossover point (°)	Max. C_l	NFD
8	2	-	1.251	-8.08
8	5	11.29	1.345	-12.55
8	8	11.99	1.432	-15.90
8	11	11.29	1.441	-17.73
13	2	-	1.325	10.64
13	5	-	1.425	18.20
13	8	-	1.448	22.49
13	11	6.59	1.493	18.91

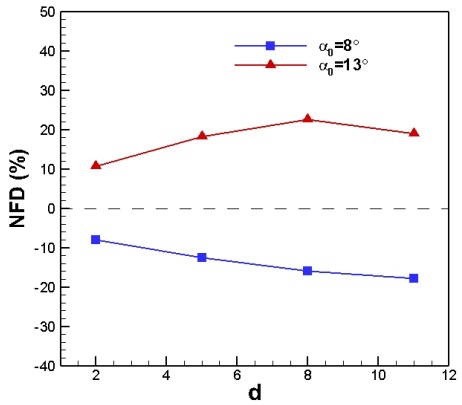

Fig. 8. Normal force defect vs. amplitude for two different cases.

is descending which points out the expansion of the counterclockwise part with respect to the whole area of the hysteresis is nonlinear.

As illustrated in Fig. 8, when the mean AOA is 13°, the airfoil motion is in dynamic stall region. Hence, the drop in lift curves is expected at high AOAs. As seen in Fig. 7(b), more severe drop in lift coefficient is observable at higher amplitude of oscillation. This makes the hysteresis loop wider and consequently, larger values of the NFD would be attained. However, when the amplitude of oscillation is 11°, the flow has enough time to reattach to the surface of the airfoil in downstroke motion. As a result, the lift value rises again and the "Fig. 8" occurs in hysteresis loop. In this case, the negative value of the counterclockwise part decreases the numerator of the Eq. (2) and hence, the NFD drops slightly.

4. Conclusions

In this study, we experimentally investigated the effects of reduced frequency, mean AOA and amplitude on lift coefficient hysteresis for a harmonically oscillating wind turbine airfoil. Qualitative analysis of the shapes of lift curves as well as quantitative study of the maximum lift coefficient, the crossover point in dynamic loop and the NFD of the airfoil in different conditions were conducted herein.

Our investigation reveals that k, d, mean AOA are of great importance in aerodynamic performance of a wind turbine airfoil. The comparison of load curves suggested that the mentioned parameters have a great impact on the slope and width of lift curves, "Fig. 8" occurrence, displacement of crossover point and the direction of the rotation. In addition, for better analysis of the hysteresis loops, a parameter named NFD was defined to study the lift curves quantitatively.

The measured values demonstrated that the slope and width of the hysteresis loops are highly affected by reduced frequency. At near stall region, higher reduced frequencies lead to drop in the slope of the lift curves. The widths of the loops, however, grow slightly and maximum lift is attained at higher AOAs. Dynamic stall can probably occur if the AOA is high enough where the flow separates from the upper surface of the airfoil and the DSV convects downstream. This leads to "Fig. 8" occurrence, representing flow-reattachment in downstroke motion. The crossover point moves forward as the reduced frequency goes up. In post-stall region, however, the flow cannot reattach to the airfoil surface and as a result, no intersection happens in lift loops.

In addition, the mean AOA of an oscillating airfoil has a great impact on the lift hysteresis. Increase in mean AOA makes the airfoil undergo dynamic stall due to high AOAs. As a result, the flow separation leads to reduction in the slope of the lift curves. Also, at the existence of dynamic stall, the "Fig. 8" shape occurs where at higher mean AOAs, the crossover point moves backward representing a delay in reattachment in downstroke motion. In contrast to the first two parameters, the amplitude of oscillation does not make any change in the slope of the lift curves. Nevertheless, higher amplitudes shift the curves downward which can be attributed to the portion of the attached-flow area on the upper surface of the airfoil which would be shortened by increase of amplitude.

Moreover, a new parameter called NFD was studied for better analysis of lift hysteresis loops. Generally, in near-stall region as the reduced frequency increases, the value of NFD decreases while in post-region, the NFD increases to large positive values by increase of reduced frequency. Also, the results revealed the fact that in dynamic stall occurrence, the maximum NFD is attained when the reattachment cannot take place entirely in downstroke motion.

Nomenclature

α : Angle of attack (AOA)
α_0 : Mean AOA
C_n : Normal force coefficient
d : Amplitude
f : Pitching frequency
ξ : Normal force defect (NFD)
k : Reduced frequency

References

[1] J. G. Leishman, Challenges in modelling the unsteady aero-

dynamics of wind turbines, *Wind Energy*, 5 (2002) 85-132.
[2] C. P. Butterfield, *Aerodynamic pressure and flow-visualization measurement from a rotating wind turbine blade*, Solar Energy Research Inst., Golden Co., USA (1988).
[3] Z. Jin, Q. Dong and Z. Yang, A stereoscopic PIV study of the effect of rime ice on the vortex structures in the wake of a wind turbine, *Journal of Wind Engineering and Industrial Aerodynamics*, 134 (2014) 139-148.
[4] T. Theodorsen and W. Mutchler, General theory of aerodynamic instability and the mechanism of flutter, Technical report, *SEE NACA-ARR-1935* (1935).
[5] K. W. McAlister, L. W. Carr and W. J. McCroskey, *Dynamic stall experiments on the NACA 0012 airfoil*, NASA (1978).
[6] W. McCroskey, K. McAlister, L. Carr and S. Pucci, *An experimental study of dynamic stall on advanced airfoil sections, Summary of the experiment*, NASA, 1 (1982).
[7] W. J. McCroskey, *The phenomenon of dynamic stall*, National Aeronuatics and Space Administration Moffett Field Ca Ames Research Center (1981).
[8] W. J. McCroskey, Unsteady airfoils, *Annual Review of Fluid Mechanics*, 14 (1982) 285-311.
[9] Q. Wang and Q. Zhao, Experiments on unsteady vortex flowfield of typical rotor airfoils under dynamic stall conditions, *Chinese Journal of Aeronautics,* 29 (2016) 358-374.
[10] M. Masdari, M. Jahanmiri, M. R. Soltani, A. Tabrizian and M. Gorji, Experimental investigation of a supercritical airfoil boundary layer in pitching motion, *Journal of Mechanical Science and Technology*, 31 (2017) 189-196.
[11] A. R. Davari, Wake structure and similar behavior of wake profiles downstream of a plunging airfoil, *Chinese Journal of Aeronautics* (2017).
[12] J. Yu, T. Leu and J.-J. Miau, Investigation of reduced frequency and freestream turbulence effects on dynamic stall of a pitching airfoil, *Journal of Visualization*, 20 (2017) 31-44.
[13] D. Rival, T. Prangemeier and C. Tropea, The influence of airfoil kinematics on the formation of leading-edge vortices in bio-inspired flight, *Experiments in Fluids*, 46 (2009) 823-833.
[14] M. K. Phan and J. Shin, Numerical investigation of aerodynamic flow actuation produced by surface plasma actuator on 2D oscillating airfoil, *Chinese Journal of Aeronautics*, 29 (2016) 882-892.
[15] R. F. Maezabadi, M. Masdari and M. Soltani, Application of artificial neural network for the prediction of pressure distribution of a plunging airfoil, *The International Conference on Fluid Mechanics, Heat Transfer and Thermodynamics (FMHT2008),* Paris, França (2008).
[16] G. Zhao and Q. Zhao, Parametric analyses for synthetic jet control on separation and stall over rotor airfoil, *Chinese Journal of Aeronautics*, 27 (2014) 1051-1061.
[17] M. Seyednia, S. Vakilipour and M. Masdari, Numerical investigation of dynamic stall over a wind turbine pitching airfoil by using OpenFOAM, *World Academy of Science, Engineering and Technology, International Journal of Mechanical, Aerospace, Industrial, Mechatronic and Manufacturing Engineering*, 11 (2017) 1475-1486.
[18] D. Poirel, V. Metivier and G. Dumas, Computational aeroelastic simulations of self-sustained pitch oscillations of a NACA0012 at transitional Reynolds numbers, *Journal of Fluids and Structures*, 27 (2011) 1262-1277.
[19] T. Lee and P. Gerontakos, Investigation of flow over an oscillating airfoil, *Journal of Fluid Mechanics*, 512 (2004) 313-341.
[20] G. Martinat, M. Braza, Y. Hoarau and G. Harran, Turbulence modelling of the flow past a pitching NACA0012 airfoil at 105 and 106 Reynolds numbers, *Journal of Fluids and Structures*, 24 (2008) 1294-1303.
[21] K. Lu, Y. Xie, D. Zhang and J. Lan, Numerical investigations into the asymmetric effects on the aerodynamic response of a pitching airfoil, *Journal of Fluids and Structures*, 39 (2013) 76-86.
[22] K. Gharali and D. A. Johnson, Dynamic stall simulation of a pitching airfoil under unsteady freestream velocity, *Journal of Fluids and Structures*, 42 (2013) 228-244.
[23] D. R. Williams, X. An, S. Iliev, R. King and F. Reißner, Dynamic hysteresis control of lift on a pitching wing, *Experiments in Fluids*, 56 (2015) 112.
[24] A. Choudhry, M. Arjomandi and R. Kelso, Methods to control dynamic stall for wind turbine applications, *Renewable Energy*, 86 (2016) 26-37.
[25] G. H. Yu, X. C. Zhu and Z. H. Du, Numerical simulation of a wind turbine airfoil: Dynamic stall and comparison with experiments, *Proceedings of the Institution of Mechanical Engineers, Part A: Journal of Power and Energy*, 224 (2010) 657-677.

Mehran Masdari is an Assistant Professor at University of Tehran. He is holding Bsc. Eng., M.Sc. and Ph.D. degrees in Aerodynamics from Sharif University of Technology. He published more than 50 scientific papers in English and Persian. He has 15 years of job experience both in industry and academic fields. Various aerospace courses and student projects were conducted by him. His research interests are Transitional flows, Applied aerodynamics, Experimental Fluid Dynamics, Particle image velocimetry (PIV), Bluff body wakes, Turbulent boundary layer, Wind Engineering, Mechanical Engineering, Fluid Mechanics, Aerodynamics, Turbomachinery, Turbulence, Wind turbine, Vertical Axis Wind Turbine (VAWT), Micro Air Vehicles, Fluid Mechanics, Aerospace Engineering, Fluid Dynamics, Wind Tunnel Testing, Neural Network and Data Processing. E-mail: m.masdari@ut.ac.ir.